Thickness dependence of degree of spin polarization of electrical current in permalloy thin films

Mohammad Haidar* and Matthieu Bailleul†

IPCMS and NIE, UMR 7504 CNRS-Université de Strasbourg, 23 rue du Loess, BP 43, 67034 Strasbourg Cedex 2, France

(Received 7 March 2013; revised manuscript received 21 June 2013; published 23 August 2013)

Spin-polarized electrical transport is investigated in $Al_2O_3/Ni_{80}Fe_{20}/Al_2O_3$ thin films for permalloy thickness between 6 and 20 nm. The degree of spin polarization of the current flowing in the plane of the film is measured through the current-induced spin-wave Doppler shift. We find that it decreases as the film thickness decreases from 0.63 at 20 nm to 0.42 at 6 nm. This decrease is attributed to a spin depolarization induced by the film surfaces. A model is proposed which takes into account the contributions of the different sources of electron scattering (alloy disorder, phonons, thermal magnons, grain boundaries, film surfaces) to the measured spin-dependent resistivities.

DOI: 10.1103/PhysRevB.88.054417 PACS number(s): 75.76.+j, 73.50.−h, 75.30.Ds, 85.75.−d

I. INTRODUCTION

The flow of a spin-polarized current through a nonuniform magnetization distribution is able to transfer angular momentum to the local magnetization.[1,2] This spin-transfer torque is now used in a number of spintronic devices, in particular those involving current-induced domain-wall motion.[3] The degree of spin polarization of the electrical current, defined as the contrast between the currents carried by the majority and minority electrons ($P = \frac{J_\uparrow - J_\downarrow}{J_\uparrow + J_\downarrow}$), is an essential parameter controlling the performance of these devices. In the early days of spintronics, the contribution of the impurities to P was extracted indirectly from low temperature resistance measurements on bulk dilute alloys.[4] However, these estimates are not directly applicable to the very thin ferromagnetic films used for spintronic devices in which additional sources of electron scattering contribute to P. In particular, it is expected that film surfaces play an important role as soon as the film thickness becomes comparable to the bulk electron mean-free path.[5] Although some information could be extracted indirectly from giant magnetoresistance measurements,[6,7] there is no accurate study of the influence of film surfaces on the degree of spin polarization. In order to address this question, we have measured the film thickness dependence of P, resorting to the technique of the current-induced spin-wave Doppler shift (CISWDS) which gives a direct access to it.[8] When a dc current I passes along a ferromagnetic metal strip of width w and thickness t, the spin-transfer torque modifies the propagation of a spin wave of wave vector k in the form of a Doppler shift Δf_{Dop} of the frequency f of the spin wave which writes

$$\Delta f_{\mathrm{Dop}} = -\frac{\mu_B}{2\pi e}\frac{P}{M_s}\frac{I}{tw}k, \qquad (1)$$

where μ_B is the Bohr magneton, e is the magnitude of the electron charge, and M_s is the saturation magnetization. After our initial measurement on a permalloy film at room temperature,[8] the CISWDS technique has been extended to low temperature,[9] to other materials,[10,11] and to time-domain measurements.[12] In this paper we investigate the CISWDS as a function of the film thickness in a very common system of spintronics, namely polycrystalline permalloy films of thickness between 6 and 20 nm. The measured thickness dependence of P is interpreted within a modified two-current model accounting for all the electron scattering processes relevant for these films.

II. EXPERIMENTAL SETUP

Permalloy (Py) films of thickness 6, 10, and 20 nm sandwiched by Al_2O_3 layers were grown by magnetron sputtering on silicon substrates [Fig. 1(a)]. For each film thickness, we fabricated CISWDS devices which comprises a ferromagnetic strip of width $w = 8\ \mu$m, a pair of antennas with meander shape allowing the excitation and the detection of spin waves with a wave vector $k = 3.86\ \mu\mathrm{m}^{-1}$, and four dc pads serving to pass the dc current I through the ferromagnetic strip and to measure its resistance [Fig. 1(b)]. The propagating spin-wave spectroscopy measurements are performed as described in Refs. 13–15. In the present work, the external magnetic field $\mu_0 H_0 = 28$ mT is applied in the plane of the film perpendicular to the strip so that the spin waves propagate in the so-called magnetostatic surface wave (MSSW) configuration.[16] Compared to the magnetostatic forward volume waves (MSFVW) used in our first report,[8] MSSWs have the advantage of providing propagating spin-wave signals of higher amplitudes and of requiring a lower external field. This is at the price of an increased complexity for signal analysis. Indeed, MSSWs are known to be nonreciprocal, which means that a wave propagating in one direction have different characteristics (signal amplitude, mode profile, frequency) than the counterpropagating wave.[17] Due to these nonreciprocal features, the method we have used to extract the CISWDS for MSFVW, i.e., compare the frequency of counterpropagating spin waves at a given current,[8] cannot be used. We will see below how the MSSW nonreciprocities show up in our measurements and how the CISWDS can be extracted in their presence.

III. EXPERIMENTAL RESULTS

A. Propagating spin-wave signals

Let us first describe the signals measured in the absence of dc current. The solid curve in Fig. 2(a) shows the imaginary part of the mutual inductance ΔL_{21}[18] which corresponds to spin waves propagating from antenna 1 to antenna 2 [$+k$ on Fig. 1(b)]. The dashed curve shows the mutual inductance

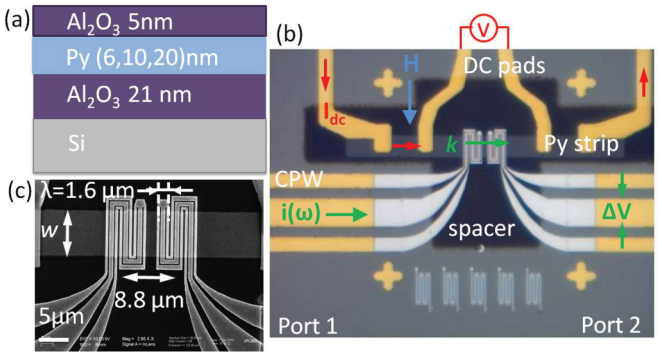

FIG. 1. (Color online) (a) Film stack. (b) Optical microscope image of the CISWDS device. One recognizes the strip ion milled from this stack, the four dc pads and the two coplanar waveguides (Ti 10 nm/Au 60 nm), the insulating spacer (SiO_2 80 nm), and the two spin-wave antennas (Ti 10 nm/Al 120 nm). The conventions used in the text for the directions of positive k, I, and H are shown. (c) Scanning electron microscope image showing the meander shape of the antennas.

ΔL_{12} (spin waves propagating from antenna 2 to antenna 1, $-k$). One sees immediately that the amplitude for $-k$ is about three times larger than that for $+k$. This amplitude nonreciprocity is a specific feature of MSSWs which has already been observed both in garnet[19] and permalloy[20–22] films. It originates from the fact that the polarization of the dynamical magnetization matches better the polarization of the antenna field for one direction than for the other [the MSSW amplitude is governed by a combination between the in-plane and out-of-plane components of the antenna field, and this combination depends on the propagation direction, see Eqs. (15) and (16) in Ref. 19]. We also observe in Fig. 2(a) that the $-k$ signal is shifted 14 MHz higher in frequency than the $+k$ one. Such frequency nonreciprocity has been observed in permalloy films dissymmetrized by a metal ground plane placed close to one film surface.[23] It can be interpreted as a combination of the mode profile nonreciprocity (MSSWs have a tendency to localize close to one film surface[24]) with some asymmetry of the magnetic system with respect to the sample midplane (in the case of Ref. 23, the metal plane provides a different boundary condition than a dielectric medium). In our case, the asymmetry could come either from different surface anisotropies at the top and bottom surfaces (see Fig. 4 in Ref. 25), or from an inhomogeneous distribution of the saturation magnetization across the film thickness. As expected, both amplitude and frequency nonreciprocities are reversed when the external field is reversed (not shown).[26] To extract the CISWDS in the presence of these nonreciprocal features, we have chosen to compare measurements taken for opposite currents.

B. Current-induced spin-wave Doppler shift

Figure 2(b) shows the current-induced frequency shifts at $|I| = 7.5$ mA: For $+k$ the $-I$ curve lies at a higher frequency than the $+I$ one [$\delta f_{21} = f_{21}(-I) - f_{21}(+I) = +7$ MHz], whereas for $-k$ the $-I$ curve lies at a lower frequency than the $+I$ one [$\delta f_{12} = f_{12}(-I) - f_{12}(+I) = -2.5$ MHz]. The signs of the observed shifts are in agreement with the CISWDS

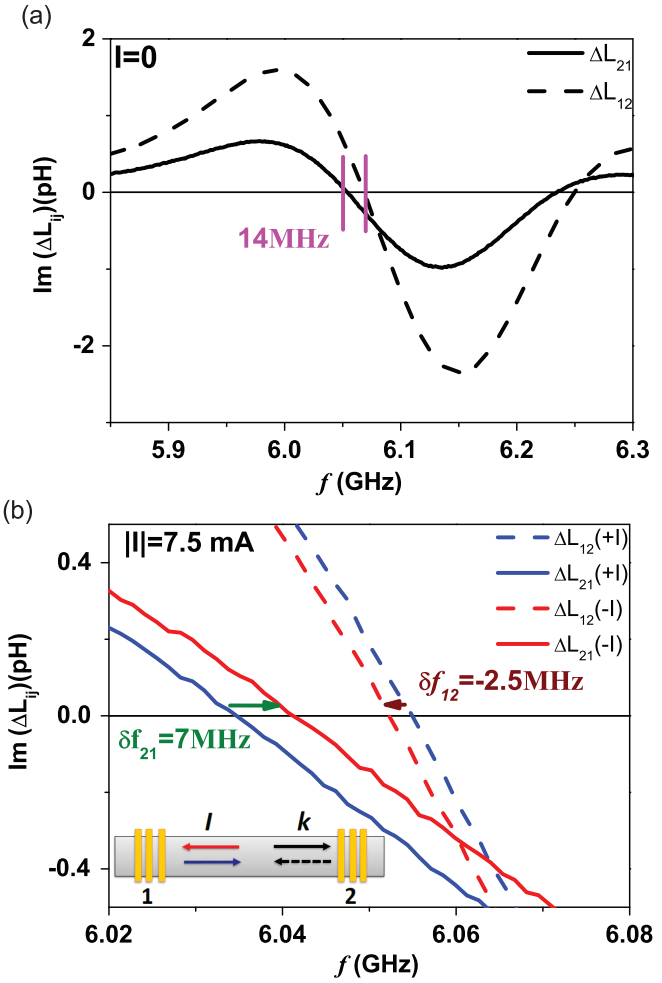

FIG. 2. (Color online) (a) Imaginary part of the mutual inductance signals ΔL_{12} and ΔL_{21} measured on the 10 nm device under a field of 28 mT and in the absence of dc current. (b) Same for a dc current of magnitude $|I| = 7.5$ mA. The frequency range for which the curves intersect the x axis has been zoomed in for clarity.

expected for $P > 0$, namely an increase of the frequency when the spin wave propagates along the electron flow, i.e., against the current. However, the magnitude of δf_{12} and δf_{21} are different, in contrast to what is expected for a pure Doppler effect. This indicates that another phenomenon, with a different symmetry with respect to k, also contributes to the observed current-induced shifts. We believe that the Oersted field generated by the dc current is the origin of this additional contribution: Due to an asymmetry across the film thickness, the Oersted field contribution to the spin-wave frequency does not average out strictly to zero. This contribution does not change sign when k is reversed. As expected, it does change sign when H is reversed (not shown). Finally, the current-induced spin-wave Doppler shift is extracted using the following relation:

$$\Delta f_{\mathrm{Dop}} = \frac{\delta f_{21} - \delta f_{12}}{4}, \tag{2}$$

where the δf_{ij} are the current-induced frequency shifts defined above.[27] This procedure allows one to separate the

CISWDS from the unwanted contributions associated to the MSSW nonreciprocity and to the Oersted field.[28] It avoids the reproducibility issues associated with the reversal of the external field[9] and gives an overall precision of the order of 100 kHz.

Figure 3(a) shows the values of the current-induced spin-wave Doppler shift as a function of the dc current for different film thicknesses. Interestingly, the shifts measured for a negative field (open symbols) are identical to those obtained for a positive field (closed symbols), which confirms that our procedure is capable of eliminating the two artifacts described above. For each film thickness, one obtains a clear linear dependence. From the slopes we extract the degree of spin polarization of the electrical current P using Eq. (1) together with the width w of the strip deduced from the SEM images and the product $\mu_0 M_s t$ deduced from SQUID measurements. The obtained spin polarization is plotted in Fig. 3(b) as a function of the inverse of the film thickness.[29] One recognizes a strong decrease of the polarization as the thickness decreases from $P = 0.63$ at $t = 20$ nm to $P = 0.42$ at $t = 6$ nm. The $1/t$ fit displayed as a thin line in Fig. 3(b) indicates a bulk extrapolate $P = 0.71$ and a critical thickness for which the polarization extrapolates to zero of 2.3 nm. This unexpectedly strong thickness dependence constitutes the main finding of the present paper. A natural way to interpret this result is to consider that the film surfaces tend to depolarize the electrical transport. The degree of spin polarization deduced from the CISWDS reflects actually an average across the thickness of the film. It is influenced by several sources of scattering, bulk- or surfacelike. As the film thickness decreases, the role of the film surfaces is enhanced, resulting in a lower polarization compared to bulk. In the remainder of the paper we give a quantitative explanation of this behavior.

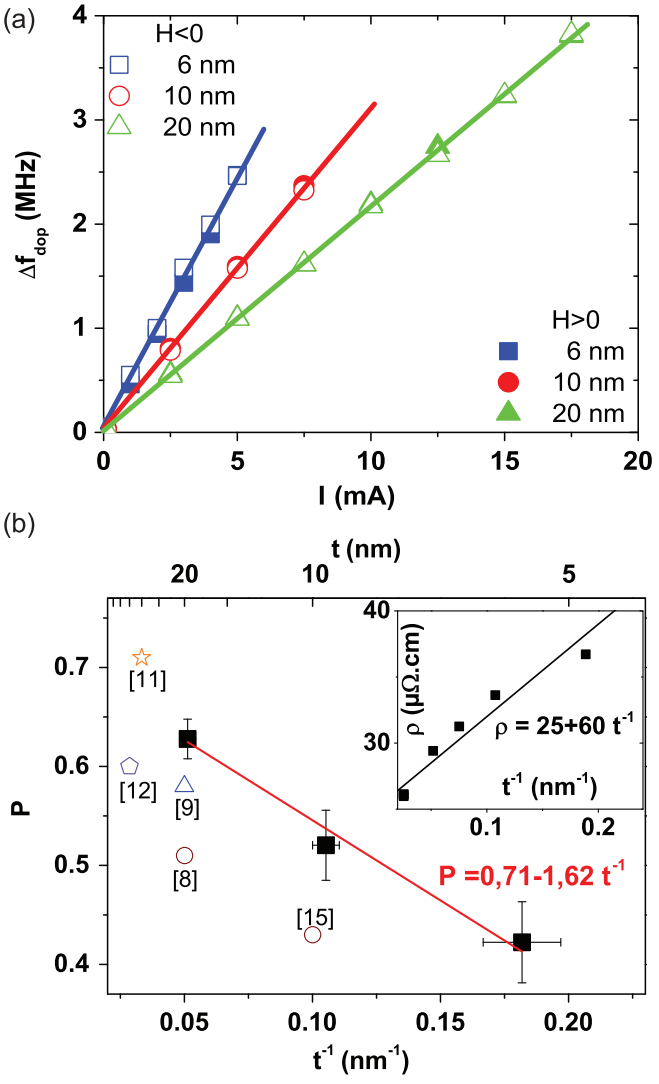

FIG. 3. (Color online) (a) Doppler frequency shift as a function of the dc current for 6, 10, and 20 nm thick films under an applied field of ±28 mT. (b) Degree of spin polarization of the electrical current as a function of the inverse of the film thickness. The inset shows the measured resistivity of each film. The colored points show published values.

IV. INTERPRETATION

To account for the polarization values of Fig. 3(b) together with the resistivity values measured on the same devices [inset in Fig. 3(b)], we propose the two-current model sketched in Fig. 4(a). The contributions of the different sources of electron scattering to the spin-dependent resistivities $\rho_\uparrow$ and $\rho_\downarrow$ of our films, namely alloy disorder, phonons, grain boundaries, and surface roughness, are assumed to sum up in series within each channel. Indeed, we believe the Mathiesen's rule to remain a reasonable approximation even for surface[5] and grain boundary[30] scattering. A spin-flip resistivity $\rho_{\uparrow\downarrow}$ is also introduced to account for spin-mixing processes.[4] Within this

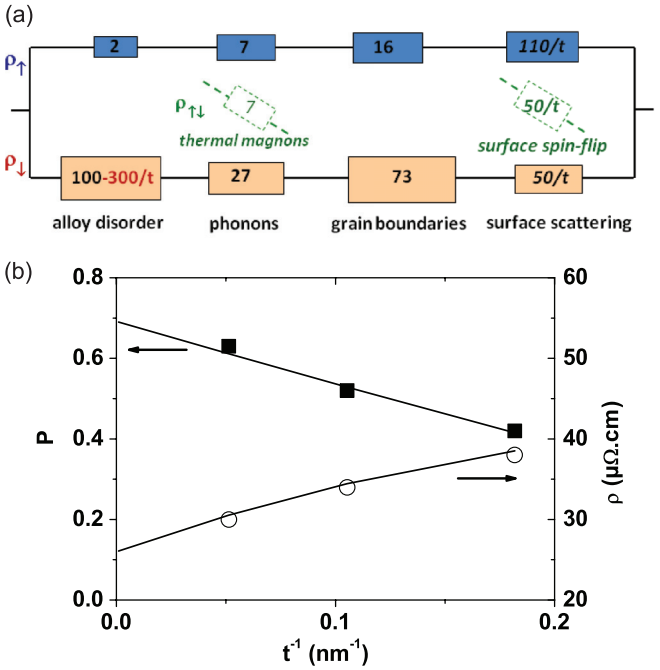

FIG. 4. (Color online) (a) Model for the spin-polarized transport in our permalloy films. (b) Spin polarization (left scale) and resistivity (right scale) versus the inverse of the film thickness. The measured values are shown as symbols and the results of the model are shown as lines.

model the resistivity and the degree of spin polarization of the current write, respectively:

$$\rho = \frac{\rho_\uparrow\rho_\downarrow + \rho_{\uparrow\downarrow}(\rho_\downarrow + \rho_\uparrow)}{\rho_\uparrow + \rho_\downarrow + 4\rho_{\uparrow\downarrow}}, \quad (3)$$

$$P = \frac{\rho_\downarrow\rho_\uparrow}{\rho_\uparrow + \rho_\downarrow + 4\rho_{\uparrow\downarrow}}. \quad (4)$$

Let us now discuss the contribution of each scattering mechanism individually, starting with the bulk mechanisms. The contribution of the alloy disorder has been estimated both experimentally[4] and theoretically.[31,32] It is known that Fe atoms in a Ni matrix act as strongly spin-dependent scattering centers.[33] Indeed, the majority electron local density of states (DOS) on Fe and Ni match very well ($\rho_\uparrow = 2\ \mu\Omega\,\text{cm}$), whereas the minority electrons DOS are very different ($\rho_\downarrow = 100\ \mu\Omega\,\text{cm}$). For the phonon contribution we use the pure nickel room temperature estimate ($\rho_\uparrow = 7\mu\ \Omega\,\text{cm}$, $\rho_\downarrow = 27\ \mu\Omega\,\text{cm}$) extrapolated from the temperature dependence of the resistivity of dilute alloys.[4] For the spin-flip resistivity induced by thermal magnons, we use the value $\rho_{\uparrow\downarrow} = 7\ \mu\Omega\,\text{cm}$ deduced from temperature-dependent CISWDS measurements.[9] Finally, we adjust the remaining bulk contributions, i.e., that of the grain boundaries, to account for the bulk extrapolates of the resistivity ($\rho_\uparrow = 25\ \mu\Omega\,\text{cm}$) and polarization ($P = 0.71$) we measure. We thus find that grain boundaries are responsible for significant contributions ($\rho_\uparrow = 16\ \mu\Omega\,\text{cm}$, $\rho_\downarrow = 73\ \mu\Omega\,\text{cm}$) with a strong spin asymmetry. This asymmetry is ascribed to the fact that minority electrons, with their complex Fermi surface, are more sensitive to details of the local atomic ordering than majority ones.[34]

Next, we discuss the contributions of the film surfaces to the electron scattering. Unless they are atomically smooth, surfaces are known to induce nonspecular (diffuse) scattering which tends to decrease the current density close to the film surface. Averaging the current density across the film thickness, this results in an increase of the film resistivity which can be approximated as $0.375(1-p)\rho_{\text{bulk}}\ell/t$, where ρ_{bulk} is the bulk resistivity, ℓ is the bulk electronic mean-free path, and p is the degree of specularity.[5] From current-in-plane giant magnetoresistance measurements, it was deduced that majority and minority electrons in permalloy have very different mean-free paths of $\ell_\uparrow = 10$ nm and $\ell_\downarrow = 0.5$ nm, respectively.[6,7] Combining those values with the bulk resistivities given above and assuming that scattering is completely diffuse ($p = 0$), one obtains the values given in the rightmost boxes in Fig. 4(a), indicating that the spin polarization for surface scattering is actually negative. This explains part of the decrease of spin polarization at smaller film thicknesses. Another part of this decrease is certainly due to a change of stoichiometry due to the selective oxidation of Fe at the film surface. Indeed, x-ray photoelectron spectroscopy indicates that approximately 1.5 nm of iron oxide is formed between the permalloy layer and the top Al_2O_3 layer, whereas the Ni remains completely metallic. As a consequence, the remaining metal layer becomes depleted in Fe ($\langle C_{\text{Fe}}\rangle = 0.2 - 0.6/t_{[\text{nm}]}$, if one assumes that 0.75 nm of iron is consumed by the oxidation). This modifies directly the alloy disorder contribution to the spin-dependent resistivities which, in good approximation, are linear with respect to C_{Fe}.[32] While the decrease of the (already small) majority resistivity can be neglected, one gets a significant decrease of the minority resistivity $\rho_{\downarrow[\mu\Omega\,\text{cm}]} = 500C_{\text{Fe}} = 100 - 300/t_{[\text{nm}]}$ [bottom leftmost box in Fig. 4(a)]. Finally, we find it necessary to include a third ingredient, namely a thickness dependent spin-flip electron scattering [rightmost dashed box in Fig. 4(a)] to account for the decrease of spin polarization at smaller film thicknesses. While the origin of this contribution is not clear at the moment, one is tempted to relate it to some spin disorder at the interface between the permalloy and the iron oxide (presumably in an antiferromagnetic phase), similar to what has been observed in over-oxidized magnetic tunnel junctions.[35]

Figure 4(b) illustrates the good agreement between the measured values of P and ρ and those obtained from Eq. (3) using the model of Fig. 4(a). Obviously the modeling we propose contains many approximations and the numbers given in each box are to be taken with caution. However, we believe that the general picture is robust because significant discrepancies appear as soon as one removes one of the ingredients of the model. Before we conclude, let us remind these ingredients: (i) a robust strongly spin-polarized alloy disorder contribution, (ii) a contribution from thermal excitations (phonons and thermal magnons) which tend to depolarize moderately the electrical current, (iii) a significant contribution from grain boundaries which is also quite strongly spin polarized, and (iv) a contribution from diffuse surface electron scattering, which in our case has a small negative spin polarization. We also identified two other effects, namely (v) depletion of iron and (vi) surface spin-flip scattering which we relate to surface oxidation and which might be specific to the film stack investigated. In our model surface effects are included as first-order corrections to the spin-dependent film resistivities. An interesting improvement of this approach would be a STT theory accounting for the inhomogeneities of the spin-polarized current distribution induced by surface scattering.

V. CONCLUSION

To conclude, our study demonstrates the influence of surface effects on the spin polarization of the current flowing in the plane of a thin ferromagnetic metal film. We believe such effects should be taken into account for spin-transfer torque experiments carried out in such a geometry. More generally, we believe that our procedure, which combines CISWDS and resistivity measurements with a detailed two-current model analysis, is the relevant one to identify the physical mechanisms governing the spin-dependent resistivities. From that point of view, systematic investigations of this kind could be very useful for the optimization of new film stacks for future STT applications.

ACKNOWLEDGMENTS

We thank the STnano staff for their assistance in nanofabrication, M. Romeo and P. Bernhardt for the XPS measurements, and F. Gautier, Y. Henry, O. Bengone, and M. Kostylev for stimulating discussions. This work was supported by the ANR (NanoSWITI, ANR-11-BS10-003).

*mohammad.haidar@hotmail.fr
†matthieu.bailleul@ipcms.unistra.fr

[1] L. Berger, Phys. Rev. B **54**, 9353 (1996).
[2] J. Slonczewski, J. Magn. Magn. Mater. **159**, L1 (1996).
[3] S. S. P. Parkin, M. Hayashi, and L. Thomas, Science **320**, 19 (2008).
[4] I. Campbell and A. Fert, in *Ferromagnetic Materials*, Vol. 3, edited by E. P. Wohlfarth (North-Holland, Amsterdam, 1982).
[5] E. Sondheimer, Adv. Phys. **1**(1), 1 (1952).
[6] B. Dieny, Europhys. Lett. **17**, 261 (1992).
[7] B. A. Gurney, V. S. Speriosu, J.-P. Nozieres, H. Lefakis, D. R. Wilhoit, and O. U. Need, Phys. Rev. Lett. **71**, 4023 (1993).
[8] V. Vlaminck and M. Bailleul, Science **322**, 410 (2008).
[9] M. Zhu, C. L. Dennis, and R. D. McMichael, Phys. Rev. B **81**, 140407(R) (2010).
[10] M. Zhu, B. D. Soe, R. D. McMichael, M. Carey, S. Maat, and J. Childress, Appl. Phys. Lett. **98**, 072510 (2011).
[11] R. Thomas, M. Zhu, C. L. Dennis, and R. D. McMichael, J. Appl. Phys. **110**, 033902 (2011).
[12] K. Sekiguchi, K. Yamada, S.-M. Seo, K.-J. Lee, D. Chiba, K. Kobayashi, and T. Ono, Phys. Rev. Lett. **108**, 017203 (2012).
[13] V. Vlaminck and M. Bailleul, Phys. Rev. B **81**, 014425 (2010).
[14] M. Haidar, Ph.D. Thesis, Université de Strasbourg, 2012.
[15] V. Vlaminck, Ph.D. Thesis, Université Louis Pasteur, 2008.
[16] D. Stancil and A. Prabhakar, *Spin Waves Theory and Applications* (Springer, Berlin, 2009).
[17] A. Gurevich and G. Melkov, *Magnetization Oscillations and Waves* (CRC, Boca Raton, FL, 1996).
[18] The ΔL_{ij}s are obtained by subtracting a reference signal registered at 190 mT (see measurement procedure in Ref. 13).
[19] T. T. Schneider, A. A. Serga, T. Neumann, B. Hillebrands, and M. P. Kostylev, Phys. Rev. B **77**, 214411 (2008).
[20] M. Bailleul, D. Olligs, and C. Fermon, Appl. Phys. Lett. **83**, 972 (2003).
[21] K. Sekiguchi, K. Yamada, S. M. Seo, K. J. Lee, D. Chiba, T. Kobayashi, and K. Ono, Appl. Phys. Lett. **97**, 022508 (2010).
[22] V. Demidov, M. P. Kostylev, K. Rott, P. Krzysteczko, G. Reiss, and S. Demokritov, Appl. Phys. Lett. **95**, 112509 (2009).
[23] P. Amiri, B. Rejaei, M. Vroubel, and Y. Zhuang, Appl. Phys. Lett. **91**, 062502 (2007).
[24] M. P. Kostylev, J. Appl. Phys. **113**, 053907 (2013).
[25] B. Hillebrands, Phys. Rev. B **41**, 530 (1990).
[26] More precisely, for conditions similar to those of Fig. 2(a) and for a field of -28 mT, the $-k$ signal is now three times smaller in amplitude and shifted 14 MHz lower in frequency than the $+k$ one. This reversal of the nonreciprocities as the field is reversed is consistent with our explanation involving the intrinsic amplitude and mode profile nonreciprocities of MSSWs.[17] It allows one to rule out explanations involving a right/left asymmetry in the sample (e.g., a difference between the first and the second antenna).
[27] For extracting the current-induced shifts with a high precision, we use $\delta f_{ij} = -f_{\mathrm{per}}\mathrm{Im}(R_{ij})/\pi$, where f_{per} is the period of the oscillating mutual-inductance signal and $R_{ij} = [\Delta L_{ij}(-I) - \Delta L_{ij}(+I)]/[\Delta L_{ij}(-I) + \Delta L_{ij}(+I)]$ is the contrast between the $+I$ and $-I$ complex signals.[14]
[28] Note that the mode profile nonreciprocity of MSSWs combining with the Oersted field is also expected to contribute to the current-induced frequency shift. However, for the range of thickness and wave vector investigated here, we have verified that the mode profile nonreciprocity remains very small (the difference of amplitude between the top and bottom surface is typically of the order of 1%), and that its contribution to the frequency shift could not exceed 100 kHz. This is in contrast with the case of a thicker film which will be discussed in a forthcoming paper.[36]
[29] The magnetic moment deduced from the SQUID measurement is such that $\mu_0 M_s t = 0.97[\mathrm{T}](t_{\mathrm{nominal}} - 1)[\mathrm{nm}]$, where t_{nominal} is the deposited thickness. X-ray reflectivity measurements indicates a metal thickness $t = t_{\mathrm{nominal}} - 0.5$ nm. The reduction of the magnetic moment and of the metal thickness is attributed to the selective oxidation of about 0.5 nm of Fe (see explanations in Sec. IV). The values given here have been used in Figs. 3(b) and 4(b).
[30] A. Mayadas and M. Shatzkes, Phys. Rev. B **1**, 1382 (1970).
[31] I. Mertig, R. Zeller, and P. H. Dederichs, Phys. Rev. B **47**, 16178 (1993).
[32] J. Banhart, H. Ebert, and A. Vernes, Phys. Rev. B **56**, 10165 (1997).
[33] P. E. Mijnarends, S. Sahrakorpi, M. Lindroos, and A. Bansil, Phys. Rev. B **65**, 075106 (2002).
[34] T. C. Schulthess, W. H. Butler, X.-G. Zhang, D. M. C. Nicholson, and J. M. MacLaren, Phys. Rev. B **56**, 8970 (1997).
[35] J. S. Moodera and G. Mathon, J. Magn. Magn. Mater. **200**, 248 (1999).
[36] M. Haidar, M. Bailleul, M. Kostylev, and Y. Lao (in preparation).